

Selecting and Driving Monolayer Structures through Tailored Intermolecular Interactions



Mr. T. J. Mullen



Dr. A. A. Dameron



Professor A. M. Andrews



Professor P. S. Weiss

*Thomas J. Mullen, Arrelaine A. Dameron,
Anne M. Andrews, and Paul S. Weiss**
104 Davey Laboratory
Departments of Chemistry, Physics, and
Veterinary and Biomedical Sciences
The Pennsylvania State University
University Park, PA 16802-6300, USA
Email: stm@psu.edu

Outline

1. Introduction
2. Varying the Intermolecular-Interaction Strengths within Monolayers
 - 2.1. *n*-Alkanethiolate Self-Assembled Monolayers
 - 2.2. Amide-Containing Alkanethiolate Self-Assembled Monolayers
 - 2.3. Adamantanethiolate Self-Assembled Monolayers
 - 2.4. *n*-Alkaneselenolate Self-Assembled Monolayers
3. Monolayer-Film Processing Techniques
 - 3.1. Coadsorption Preparations
 - 3.2. Postadsorption Processing
 - 3.3. Displacement Methods
4. Applications
 - 4.1. Molecular Electronics
 - 4.2. Chemical Patterning
 - 4.3. Tether and Capture of Biomolecules
5. Conclusions
6. Acknowledgments
7. References and Notes

1. Introduction

The development of self- and directed-assembly techniques is key for the fabrication of molecularly precise structures for applications ranging from biocompatible and/or bioactive systems to microelectronics.¹⁻³ These applications now demand patterned surface structures with ever smaller features down to the sub-100 nm scale; however, traditional lithographic techniques such as photolithography cannot reproducibly fabricate such

structures with molecular-scale organization.⁴ By employing a library of molecules with a spectrum of intermolecular-interaction strengths in conjunction with a variety of thin-film-processing techniques, it is becoming possible to fabricate nanometer-sized surface features with molecular precision.

To characterize chemically patterned surface structures, it is necessary to employ techniques that can distinguish features at the molecular scale. Ensemble-averaging techniques, such as Fourier transform infrared spectroscopy (FTIR) and X-ray photoelectron spectroscopy (XPS), determine the macroscopic properties and can give chemically specific information about thin films.⁵ However, these techniques lack the ability to characterize molecular-scale surface structures.⁶⁻⁹ In contrast, scanning probe techniques, such as scanning tunneling microscopy (STM) and lateral force microscopy (LFM), are localized techniques that can visualize the surfaces of chemically patterned thin films with ultrahigh resolution and are thus employed extensively in the area of molecular imaging.¹⁰⁻¹²

Over the last 10 years, we have discovered how to fabricate mixed-component self-assembled monolayers (SAMs) in order to create patterned film structures. This review outlines our efforts to develop and to apply molecules—with distinctive chemical and physical properties and with varying intermolecular-interaction strengths and surface stabilities—in patterning monolayer-film structures. In addition to employing molecules with tailored interactions, SAM coadsorption, postadsorption, and displacement processing techniques are used to create a variety of patterned films. We will highlight three applications where specifically tuned molecules and customized SAM

processing techniques are utilized: molecular electronics, chemical patterning, and biomolecular tethering. More comprehensive reviews on patterning self-assembled monolayers and methodologies to fabricate phase-separated SAMs have been published.^{13–16}

2. Varying the Intermolecular-Interaction Strengths within Monolayers

2.1. *n*-Alkanethiolate Self-Assembled Monolayers

The adsorption of *n*-alkanethiol molecules onto noble metal substrates has been studied extensively, and, therefore, the intermolecular-interaction strength of *n*-alkanethiolate SAMs will be used as a benchmark for comparing the intermolecular strengths of other monomolecular films.^{11,14,17} *n*-Alkanethiol molecules consist of a thiol head group with a hydrocarbon tail that can be tuned to have from 2 to over 20 methylene units. In general, longer-chain molecules have larger intermolecular interactions when compared to those of shorter-chain molecules due to increased van der Waals forces.^{18,19} The formation of *n*-alkanethiolate SAMs on Au{111} occurs in two steps. Initially, the thiol head groups of the *n*-alkanethiol molecules spontaneously adsorb onto the gold surface. Then, an ordering process occurs where the hydrocarbon tails interact, forming a crystalline structure with a nominally all-trans configuration.^{20,21} If the SAM is formed in solution, an additional adsorption–desorption exchange process occurs during the ordering step.²² **Figure 1A** is

a molecularly resolved STM image of a 1-dodecanethiolate (C12) SAM deposited on a Au{111} substrate via exposure to ethanolic solution for 24 h. The C12 molecules formed a hexagonally close-packed lattice (with nearest-neighbor spacings of 5.0 Å) in a ($\sqrt{3} \times \sqrt{3}$)R30° unit cell conformation with respect to the underlying gold lattice. In addition to the ($\sqrt{3} \times \sqrt{3}$)R30° unit cell, a primitive $c(4 \times 2)$ superlattice was observed and was due to an alternating azimuthal orientation of one molecule with respect to its neighbor. The C12 molecules tilt 30° with respect to the surface normal to maximize their interactions with neighboring molecules. This molecular tilt resulted in different domains of C12 molecules that were defined by substrate vacancy islands, substrate step edges, and domain boundaries.²³

2.2. Amide-Containing Alkanethiolate Self-Assembled Monolayers

Amide-containing alkanethiols, such as *N*-nonyl-3-mercaptopropionamide (1ATC9), have a hydrocarbon backbone with internal amide functionality. The amide functionality allows adjacent molecules to form hydrogen bonds between the carbonyl and amino moieties. As a result, the interaction strengths of amide-containing alkanethiolate SAMs are significantly larger than those of *n*-alkanethiolate SAMs.^{24–26} **Figure 2** shows a family of amide-containing alkanethiol molecules, including *N*-(*N'*-hexylacetamido)-3-mercaptopropionamide (2ATC6) and *N*-(*N'*-*n*-propylacetamido)acetamido)-3-mercaptopropionamide (3ATC3), where the intermolecular-interaction strength is increased by the number of amide functional groups that are buried within the monolayer.²⁷

The amide-containing alkanethiolate SAM formation process is analogous to those of *n*-alkanethiolate SAMs. Initially, the thiol head group of an amide-containing alkanethiol adsorbs onto the gold surface, followed by an ordering process dictated by the hydrocarbon tail interactions. In addition to the hydrocarbon tail interactions, the buried amide functionality imparts directionality in the molecular lattice with a strong tendency to form linear networks.²⁸ **Figure 1B** shows a molecularly resolved STM image of a 1ATC9 SAM adsorbed onto a Au{111} substrate by exposure to ethanolic solution for 24 h. The 1ATC9 molecules formed hexagonally close-packed lattices (with nearest-neighbor spacings of 5.0 Å) with features—such as unit cell conformation, substrate vacancy islands, step edges, and protruding domain boundaries—that are comparable to those of *n*-alkanethiolate SAMs. However, rather than the $c(4 \times 2)$ and related superlattice structures observed for *n*-alkanethiolate SAMs, there was a $p(3 \times 3\sqrt{3})$ superlattice due to lines of molecules that were formed via hydrogen bonding.

2.3. Adamantanethiolate Self-Assembled Monolayers

1-Adamantanethiol (AD) is based on adamantane, the smallest member of the diamondoid family, which consists of a ten-carbon cage that can be described as four fused cyclohexane rings in their chair conformations.²⁹ The intermolecular-interaction strengths of AD SAMs are considerably weaker than those of *n*-alkanethiolate SAMs due to the lattice spacings and the round topology of the molecule. As a result, AD SAMs are labile when exposed to other thiol molecules by contact, in solution, or in the vapor phase.^{30,31} **Figure 1C** shows a molecularly resolved STM image of an AD SAM deposited on a Au{111} substrate by exposure to ethanolic solution for 24 h. The AD molecules formed a hexagonally close-packed lattice (with a nearest-neighbor spacing of 6.9 Å) in a (7×7) unit cell with respect to the underlying gold lattice. These

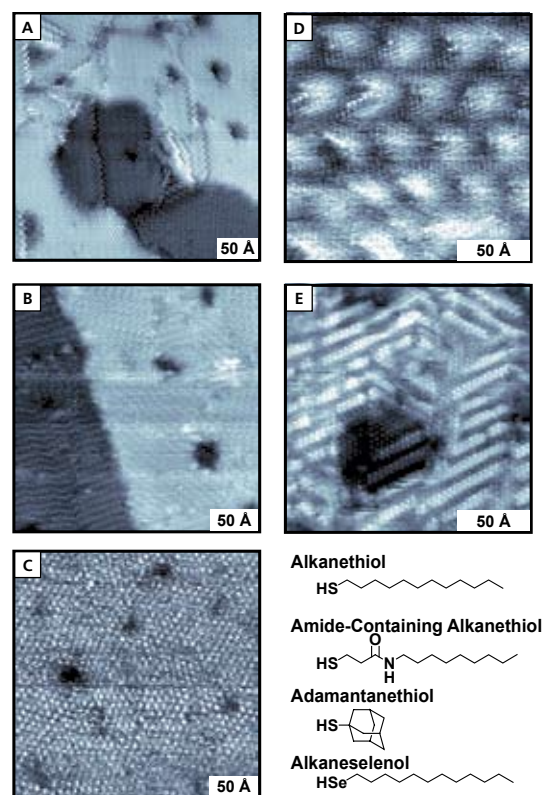


Figure 1. STM Images of Single-Component (A) 1-Dodecanethiolate ($V_{\text{sample}} = -0.75$ V, $I_{\text{tunnel}} = 3$ pA, $250 \text{ \AA} \times 250 \text{ \AA}$), (B) *N*-Nonyl-3-mercaptopropionamide ($V_{\text{sample}} = -1.0$ V, $I_{\text{tunnel}} = 3$ pA, $250 \text{ \AA} \times 250 \text{ \AA}$), (C) 1-Adamantanethiolate ($V_{\text{sample}} = -0.75$ V, $I_{\text{tunnel}} = 3$ pA, $250 \text{ \AA} \times 250 \text{ \AA}$), (D) Densely Packed Structure of 1-Dodecaneselenolate ($V_{\text{sample}} = +1.0$ V, $I_{\text{tunnel}} = 3$ pA, $165 \text{ \AA} \times 165 \text{ \AA}$), and (E) Missing-Row Structure of 1-Dodecaneselenolate ($V_{\text{sample}} = -1.0$ V, $I_{\text{tunnel}} = 3$ pA, $165 \text{ \AA} \times 165 \text{ \AA}$) SAMs Formed on Au{111} Substrates by Exposure to Ethanolic Solution for 24 h.

nearest-neighbor spacings for AD SAMs are considerably larger than those of *n*-alkanethiolate SAMs. Substrate vacancy islands and step edges observed in AD SAMs have similar structures to those of *n*-alkanethiolate SAMs; however, AD SAMs lack the large variety of domain boundaries associated with the tilt of *n*-alkanethiolate SAMs. Instead, AD SAMs have “depressed” domain boundaries (as observed in STM images) resulting from mismatched rotational domains of the AD molecules.

2.4. *n*-Alkaneselenolate Self-Assembled Monolayers

n-Alkaneselenol molecules consist of a hydrocarbon backbone with a selenol (SeH) head group. Similar to *n*-alkanethiol molecules, the length of the hydrocarbon tail, which can range from 2 to over 20 methylene units, affects the strengths of the resulting intermolecular interactions. However, *n*-alkaneselenolate SAMs have larger head group–head group interactions than those of *n*-alkanethiolate SAMs, which affects their monolayer structures. 1-Dodecaneselenolate (C12Se) SAMs form two coexisting phases, a densely packed distorted hexagonal lattice and a missing-row lattice, after exposure to a tetrahydrofuran solution for 24 h.³² **Figure 1D** shows a molecularly resolved STM image of the densely packed structure of a C12Se SAM deposited on a Au{111} substrate. The C12Se molecules in this phase formed a distorted hexagonal lattice with nearest-neighbor spacings of 4.9 Å and 5.2 Å. A moiré pattern was observed indicating that the distorted densely packed lattice was incommensurate to the underlying gold substrate (i.e., the selenolate molecules were not located on sites in registry with the Au lattice). **Figure 1E** shows a molecularly resolved STM image of the missing-row structure of a C12Se SAM deposited on a Au{111} substrate. The molecules in this phase formed a commensurate but incomplete lattice with variants of the $(\sqrt{3} \times \sqrt{3})R30^\circ$ unit cell with respect to the underlying gold lattice. The unit cell variants arise from selenolate head groups shifting between adjacent Au adsorption sites (bridge and 3-fold lattice sites). The proposed formation process of *n*-alkaneselenolate SAMs consists of two steps. Initially, *n*-alkaneselenolate molecules adsorb rapidly onto the gold surface, forming the missing-row lattice. This rapid adsorption is followed by a slow rearrangement of the selenolate head groups through adsorption of additional *n*-alkaneselenolate molecules. This rearrangement leads to the formation of the distorted hexagonal lattice. Similarly to what occurs during *n*-alkanethiolate SAM formation, the hydrocarbon tails of *n*-alkaneselenolates interact and develop into a crystalline lattice.³²

3. Monolayer-Film Processing Techniques

3.1. Coadsorption Preparations

Coadsorption combines two different adsorbate molecules in a single deposition (solution or vapor).^{33,34} If there is a sufficient difference in the intermolecular-interaction strengths between the two adsorbate molecules, then the molecules will aggregate into separated domains in order to maximize their respective intermolecular interactions. However, if there is insufficient difference in the intermolecular interactions between the two adsorbate molecules, then a mixed monolayer forms, where the two molecules are dispersed throughout the SAM.³⁵ The intermolecular interactions can be tuned by modifying the structure of the adsorbing molecule. Additionally, the interaction strengths of the coadsorbing molecules influence the adsorption affinities of the molecules. This is reflected by the surface concentrations of the two adsorbates not directly mirroring the

solution concentrations of the two species. We have demonstrated the ability to fabricate phase-separated SAMs by tailoring the terminal functional group, the hydrocarbon backbone, and the head group of the adsorbing molecule.^{28,36,37} In all cases, equilibrium structures are not reached, due to the restricted mobility of the molecules and their limited ability to exchange between the surface and the deposition medium.

Phase-separated SAMs with domains of molecules with different reactivities can be dictated by the *terminal functionality* of the two molecules that are coadsorbed. Stranick et al. demonstrated this method by fabricating phase-separated SAMs of coadsorbed 1-hexadecanethiol (C16) molecules and methyl 15-mercapto-1-pentadecanoate (C15ME) molecules.³⁸ Both of these molecules have similar hydrocarbon-chain lengths and differ only in the terminal functional groups. **Figure 3A** displays an STM image of the phase-separated SAM consisting of methyl-terminated molecules (less protruding domains) and methyl-ester-terminated molecules (more protruding domains). This and related STM images show that there are phase-separated, nanometer-scale domains of the two molecules on the surface; the domains were identified (C15ME appears more protruding) by varying the surface coverage ratios.^{39,40}

Another method of fabricating phase-separated SAMs is to coadsorb molecules that drive the formation of separated SAMs as a result of their *internal* functionalization. Smith et al. demonstrated phase-separated SAMs obtained by the internal functionalization method by the coadsorption of 1ATC9 and 1-decanethiol (C10).²⁸ **Figure 3B** shows an STM image of a phase-separated 1ATC9 (appears as a more protruding lattice) and C10 (appears as a less protruding lattice) SAM.⁴¹ Although the phase-separated SAMs had the same terminal functionality in both domains, they were separated due to different intermolecular-interaction strengths and domain stabilities. For example, the C10 domains adsorb onto the surface less strongly and desorb more readily than 1ATC9 domains.²⁷ Note that the advantage of having buried hydrogen bonds can only be exploited when the amide functionality is present in adjacent properly oriented molecules. This leads to linear hydrogen-bonding networks that result in significant effects in the monolayer structure.^{13,27,28}

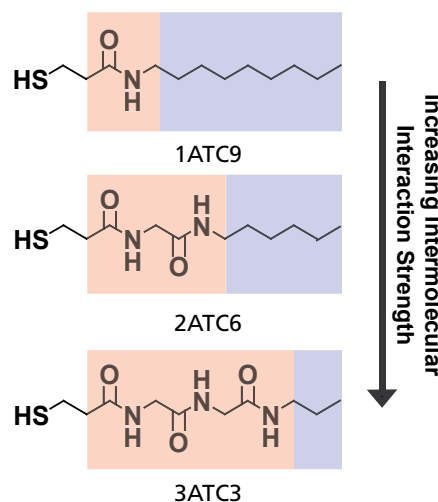


Figure 2. Amide-Containing Alkanethiol Molecules Exhibiting Increased Intermolecular-Interaction Strength as the Number of Amide Functional Groups Increases.

Head-group functionality also directs phase separation in coadsorbed SAMs.³⁷ **Figure 3C** displays an STM image of a phase-separated C12Se (more protruding regions) and C10 (less protruding regions) SAM.⁴¹ These molecules have identical terminal groups and similar hydrocarbon chain lengths, but differ in their head-group functionalities. However, unlike phase separation that is driven by terminal or internal functionality, the two lattice types of the separated SAM in **Figure 3C** have vastly different structures. The different head groups offer a method to create molecular films with separated domains that have distinct conductance differences. This quality may be useful in the design of molecular electronic devices.⁴²

Generally, the solution composition (i.e., solution mole fraction) before coadsorption dictates the surface composition (i.e., fractional surface coverage). However, the solution mole fraction is not necessarily directly reflected in the fractional surface coverage. For example, Lewis et al. varied the molar ratios of 1ATC9 and C10 in deposition solutions.²⁷ It was observed that at high concentrations of 1ATC9 the solution mole fraction and the fractional surface coverage were correlated. As the 1ATC9

concentration decreased, a dramatic and nonlinear decrease in the ratio of the fractional surface coverage to solution mole fraction was observed. This effect was attributed to the 1ATC9 molecules having larger intermolecular-interaction strengths than C10 molecules and, therefore, being stabilized on the surface by adjacent 1ATC9 molecules. Additionally, the solvation of the 1ATC9 molecules and the C10 molecules also influences the adsorption process. Molecules that are preferentially solvated or aggregated, such as 1ATC9, may not adsorb as quickly onto the surface. Moreover, as the 1ATC9 solution mole fraction decreases, the large number of solvated C10 molecules, in combination with fewer 1ATC9 molecules on the surface, stabilizes the SAM. Thus, the exchange process favors desorption of 1ATC9 and adsorption of C10 molecules.

3.2. Postadsorption Processing

One form of postadsorption processing modifies a pre-existing SAM with heat, the presence of extra thiol molecules in the vapor phase, or thiol molecules in solution.^{43–45} These modifications enable the fabrication of separated SAMs with adsorbate molecules that form mixed monolayers when coadsorbed.

Thermal annealing creates multicomponent SAMs by heating a preformed single-component SAM and subsequently exposing that SAM to another thiol. Bumm et al. employed thermal annealing to fabricate separated C12 and C10 SAMs.⁴⁵ Initially, a single-component C12 SAM was fabricated via solution deposition in ethanol for 1 h at 78 °C. The partially desorbed SAM was then immersed into an ethanolic solution of C10 for 6 h at room temperature. **Figure 4A** shows an STM image of the separated C12 and C10 SAM produced via thermal annealing. This SAM was composed of virtually defect-free islands of C12 molecules (more protruding lattice) surrounded by domains of C10 molecules (less protruding lattice), where the defect density and domain boundaries were consistent with the SAMs adsorbed at room temperature. The C10 molecules adopted the same orientation and packing as the C12 molecules in order to maximize their intermolecular interactions. Additionally, molecularly sharp domain boundaries free of physical defects were observed throughout the SAM.

Vapor-phase annealing modifies a pre-existing SAM with thiol molecules from the vapor phase. These molecules insert into defect sites—such as vacancy islands, step edges, and domain boundaries—of the preformed SAM, creating a patterned multicomponent SAM.⁴³ **Figure 4B** shows a molecularly resolved STM image of a single-component 1-octanethiolate (C8) SAM vapor-annealed with C10 for 1 h at room temperature. The more protruding lattice is attributed to C10 and the less protruding one to C8.⁴¹ From the STM image, one finds that the C10 molecules insert around the vacancy islands and domain boundaries present in the SAM. As in the case of thermal annealing, the C10 molecules adopt the same packing and orientation as the C8 molecules.

Solution-phase insertion exposes a preformed single-component SAM to thiols in solution.^{44,46,47} However, rather than a large number of molecules inserting in connected bundles at defect sites as with vapor-phase annealing, the solvated molecules tend to insert individually at defect sites of the single-component SAM. This technique can be used to isolate single molecules in order to probe their respective chemical and physical properties. For example, **Figure 4C** is an STM image of oligo(phenylene ethynylene) (OPE) molecules inserted into a C8 host SAM.⁴¹ The STM images showed that the OPE molecules (most protruding features) inserted at defect sites, such as substrate vacancy islands

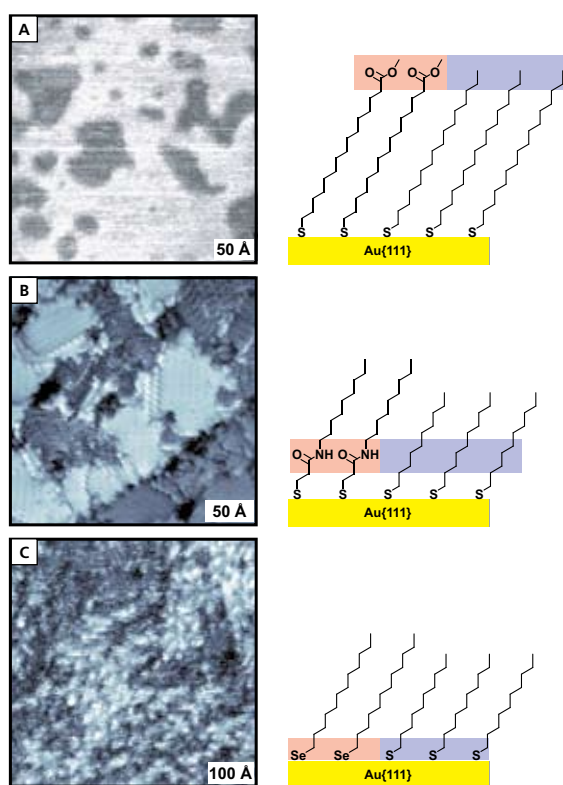


Figure 3. (A) STM Image ($V_{\text{sample}} = -1.0$ V, $I_{\text{tunnel}} = 1$ nA, $310 \text{ \AA} \times 310 \text{ \AA}$) of a Separated Methyl Ester ω -Functionalized 1-Pentadecanethiolate (More Protruding Lattice) and 1-Hexadecanethiolate (Less Protruding Lattice) SAM Formed on a Au(111) Substrate from a 75% Methyl Ester ω -Functionalized 1-Pentadecanethiol and 25% 1-Hexadecanethiol Solution (1 mM in Total Thiol). (B) STM Image ($V_{\text{sample}} = -1.0$ V, $I_{\text{tunnel}} = 1$ pA, $250 \text{ \AA} \times 250 \text{ \AA}$) of a Separated *N*-Nonyl-3-mercaptopropionamide (More Protruding Lattice) and 1-Dodecanethiolate (Less Protruding Lattice) SAM Formed on a Au(111) Substrate from an Equimolar Solution of *N*-Nonyl-3-mercaptopropionamide and 1-Decanethiol (1 mM in Total Thiol). (C) STM Image ($V_{\text{sample}} = -1.0$ V, $I_{\text{tunnel}} = 1$ pA, $500 \text{ \AA} \times 500 \text{ \AA}$) of a Separated SAM of 1-Dodecaneselenol (More Protruding Lattice) and 1-Dodecanethiolate (Less Protruding Lattice) Formed on a Au(111) Substrate from a 90% 1-Dodecaneselenol and 10% 1-Dodecanethiol Solution (1 mM Total).

and domain boundaries, and that the crystalline order of the host C8 SAM was preserved after insertion.

The relative sizes of the domains of the two lattice types of the separated SAM were determined by the postadsorption processing time and from the solution concentration of the second molecule. For example, by tailoring the OPE solution concentration and the insertion time, the number of molecules that were inserted from the solution phase into the preformed C8 SAM was controlled, allowing for single-molecule measurements to be acquired for a large number of molecules in a single STM image.⁴⁶ Additionally, solution-phase insertion techniques have been employed to isolate, to dilute optimally, and to anchor single-molecule polymer precursors to surfaces, where ring-opening polymerization can proceed to grow single polymer chains.⁴⁸ Likewise, insertion of larger bundles of tethers can be used to grow anchored polymer brushes.

3.3. Displacement Methods

Displacement employs a single-component SAM composed of molecules that are labile when exposed to other thiol molecules by contact, in solution, or in the vapor phase.^{30,31,49} As displacement occurs, ordered separated domains of both molecules can be observed until the SAM is composed entirely of the second thiolated molecule. Single-component AD SAMs are ideal for this process due to their lower density of molecule–surface bonds and low intermolecular-interaction strengths as compared to those of *n*-alkanethiolate SAMs.

Solution displacement exposes a single-component SAM to a solvated thiol molecule. The solvated molecules insert at defect sites of the pre-existing SAM and grow into domains until the preformed SAM is displaced completely.³¹ **Figure 5A** is an STM image of a separated C12-and-AD SAM created via solution displacement for 1 h. The most protruding lattice that originates at the substrate defects is attributed to C12, while the less protruding lattice is attributed to AD.⁴¹ As discussed above, the lattice spacings of the AD molecules are significantly different from those of the C12 lattice. This difference, together with the differences in the apparent heights of the two lattices, simplifies identification of the different regions in the separated C12-and-AD SAM. At long displacement times, the separated SAM becomes composed entirely of C12 molecules.

Vapor displacement exposes a single-component SAM to thiol molecules in the vapor phase. The molecules in the vapor phase insert at defect sites and grow into domains until completely displacing the preformed AD SAM.³⁰ This is in contrast to what occurs during vapor-phase annealing, where the inserted molecules do not replace the existing preformed SAM completely. **Figure 5B** is an STM image of a separated C10-and-AD SAM created by vapor displacement of AD with C10 for 15 min. The more protruding lattice is attributed to C10 domains and the less protruding one to AD domains.⁴¹ Substrate defects, such as vacancy islands and substrate step edges are also present. Higher surface coverages by C10 have been observed for vapor displacement than for solution displacement when using similar displacement times and concentrations.

Contact displacement places an existing SAM into contact with an elastomeric stamp that is coated with molecules to be patterned; the molecules on the stamp displace the existing SAM only in places where the stamp and substrate are in contact.^{49,50} **Figure 5C** is an STM image of a separated C10-and-AD SAM fabricated by contact displacement. The more protruding regions are attributed to C10 molecules and the less protruding ones to AD molecules.⁴¹ The entire substrate was contacted with an

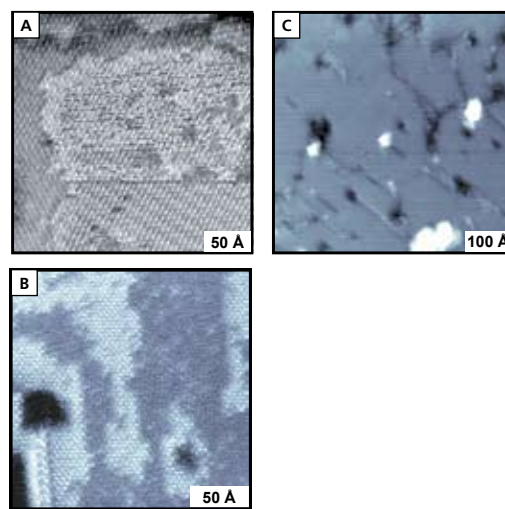


Figure 4. (A) STM Image ($V_{\text{sample}} = -1.0$ V, $I_{\text{tunnel}} = 10$ pA, 250 Å \times 250 Å) of a Separated 1-Decanethiolate (Less Protruding Lattice) and 1-Dodecanethiolate (More Protruding Lattice) SAM Fabricated on a Au{111} Substrate by *Thermal Annealing* of a 1-Decanethiolate SAM and Subsequent Exposure to an Ethanolic Solution of 1-Dodecanethiol for 5 min. (B) STM Image ($V_{\text{sample}} = -1.0$ V, $I_{\text{tunnel}} = 2$ pA, 200 Å \times 200 Å) of a Separated 1-Octanethiolate (Less Protruding Lattice) and 1-Decanethiolate (More Protruding Lattice) SAM Fabricated on a Au{111} Substrate by *Vapor Annealing* of a Single-Component 1-Octanethiolate SAM with 1-Dodecanethiol. (C) STM Image ($V_{\text{sample}} = -1.0$ V, $I_{\text{tunnel}} = 2$ pA, 500 Å \times 500 Å) of a 1-Octanethiolate SAM *Solution-Inserted* with Oligo(Phenylene Ethynylene) Molecules (Protrusions) for 5 min on a Au{111} Substrate.

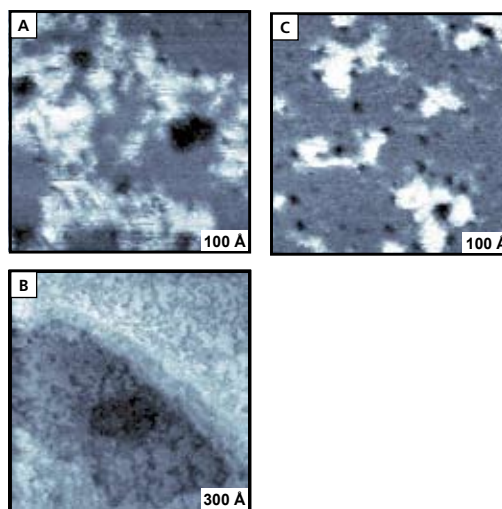


Figure 5. (A) STM Image ($V_{\text{sample}} = -1.2$ V, $I_{\text{tunnel}} = 5$ pA, 500 Å \times 500 Å) of a Preformed 1-Adamantanethiolate SAM on a Au{111} Substrate That Was *Solution-Displaced* by 1 mM 1-Dodecanethiol for 1 h. The More Protruding Lattice Is Attributed to 1-Dodecanethiolate and the Less Protruding One to 1-Adamantanethiolate. (B) STM Image ($V_{\text{sample}} = -1.0$ V, $I_{\text{tunnel}} = 2$ pA, 1500 Å \times 1500 Å) of a Preformed 1-Adamantanethiolate SAM on a Au{111} Substrate That Was *Vapor-Displaced* by Neat 1-Decanethiol for 15 min. The More Protruding Lattice Is Attributed to 1-Decanethiolate and the Less Protruding One to 1-Adamantanethiolate. (C) STM Image ($V_{\text{sample}} = -1.0$ V, $I_{\text{tunnel}} = 1$ pA, 500 Å \times 500 Å) of a Preformed 1-Adamantanethiolate SAM That Was *Contact-Displaced* with 75 mM Ethanolic 1-Decanethiol for 2 min. The More Protruding Lattice Is Attributed to 1-Dodecanethiolate, and the Less Protruding One to 1-Adamantanethiolate.

unpatterned stamp inked with C10 molecules. Displacement was observed initially at defects within the SAM and, as the contact time was increased, the size of the C10 domains increased until the SAM was completely composed of C10 molecules.

Similar to postadsorption methods, there is a large array of molecules that can be employed for displacement. The molecule that makes up the sacrificial SAM is not limited to AD, but it must be sufficiently labile that it can be displaced when exposed to another thiol molecule. Additionally, the molecules that displace the existing SAM must have sufficient intermolecular-interaction strengths to form domains. Weiss's group observed striped regions rather than patches of molecules when hexanethiol (C6) was used as the displacing molecule.³¹ These striped regions were attributed to the lower intermolecular-interaction strength associated with the shorter-chain C6 molecules. Additionally, vapor- and contact-displacement processing produced separated SAMs without solution, allowing for the use of molecules that could not be patterned before due to solubility problems.³⁰

4. Applications

4.1. Molecular Electronics

Semiconductor microelectronic devices have physical-size limitations; therefore, new approaches are needed to fabricate smaller and faster devices. Electron transport through a single molecule is the ultimate limitation, but little is understood at a fundamental level of the behavior, operation, and optimization of the functional molecules in molecular electronics. By modifying the interaction strength of both individual molecules and the surrounding matrix, and tailoring the local environment through SAM processing techniques, the behavior of molecular devices has been modified in order to test and elucidate their respective mechanisms. Solution insertion techniques have been developed specifically to isolate single molecules within a host matrix and

to characterize their electronic and structural properties with STM.^{44,46,51}

The stochastic switching in single OPE molecules was mediated by tuning the intermolecular-interaction strength between the molecules and the host matrix. Lewis et al. tailored the host matrix by employing an amide-containing alkanethiolate SAM rather than an *n*-alkanethiolate SAM.^{52,53} For an unfunctionalized OPE molecule, stochastic switching of the OPE molecule was observed; no hydrogen bonding between the OPE and the matrix was possible, but the tightness of the matrix affected the switching rate (**Figure 6A**).⁵³ However, when a nitro group (NO₂) was included as part of the OPE molecule and the proper matrix was selected, bias-dependent switching was observed and attributed to the nitro group of the functionalized OPE molecule interacting with the applied electric field and stabilized by hydrogen bonding with the amide-containing host matrix (**Figure 6B**).^{52,53} This strategy of modifying the chemical functionality of both the molecular device and the host matrix demonstrated the ability to modulate the switching behavior of molecular devices.

In addition to tailoring the intermolecular interactions of the SAM, the stochastic switching activity of single-molecule devices was controlled by modifying the local environment via molecular processing techniques.⁴⁷ The order and density of the host matrix film played a crucial role in mediating the stochastic switching activity of OPE molecules.⁴⁶ Donhauser et al. employed vapor-phase annealing of C12 molecules to increase the density of the host matrix around single OPE molecules that had been solution-inserted into preformed C10 SAMs.⁴³ **Figure 7A** shows a diagram of the vapor-phase annealing of C12 into a preformed C10 SAM that had previously had OPE molecules inserted in it from solution. The C12 molecules in the vapor phase inserted around the defect sites where the OPE molecules were already adsorbed. **Figure 7B** shows a representative STM image of this type of SAM. The red arrow indicates where the OPE molecule inserted into the host matrix; the most protruding domains surrounding the defects were attributed to C12 molecules and the less protruding domains on the terraces were attributed to C10 molecules.⁴¹ The switching rate of the OPE molecules and the number of OPE molecules that switched were observed to be significantly lower than the switching rate of OPE molecules that were solution-inserted into a C10 SAM without vapor-phase annealing. This chemical processing of the C10 SAM allowed the switching activity of the OPE molecules to be controlled.

From experiments that tuned the intermolecular interactions of the OPE molecules and the host matrix SAM, and those that modified the local environment of the host SAM via molecular processing techniques, the conductance switching mechanism was determined to be caused by a change in the hybridization of the OPE molecules that occurs with a change in the molecule-substrate contact. Moore et al. engineered OPE molecules with varying structures designed to test several proposed switching mechanisms.⁵⁴ Although this work supports the proposed mechanism that switching is due to a change in the hybridization of the OPE molecule-substrate bond, a more detailed discussion of it is beyond the scope of this review.

4.2. Chemical Patterning

Chemical patterning techniques are straightforward and versatile methods to direct the location of molecules on the micro- to nanometer scale.¹⁵ Several approaches that will be discussed below include soft lithography and artificial separation methodologies. Soft-lithography techniques, such as microcontact printing and

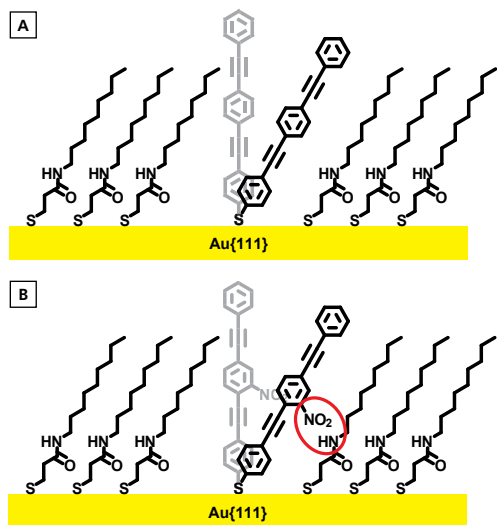


Figure 6. (A) Schematic of an Unfunctionalized Oligo(Phenylene Ethynylene) Molecule Inserted into a Preformed *N*-Nonyl-3-mercaptopropionamide SAM Showing How the Inserted Molecule Switches Stochastically but Does Not Form Hydrogen bonds with the Amide Functional Group of the *N*-Nonyl-3-mercaptopropionamide SAM. (B) Schematic of an Oligo(Phenylene Ethynylene) Molecule Functionalized with a Nitro Group (NO₂) Inserted into a Preformed *N*-Nonyl-3-mercaptopropionamide SAM Showing the Hydrogen Bonding (Red Oval) between the Nitro and the Amido Functional Groups.

dip-pen nanolithography, fabricate chemical features on a substrate without the direct assistance of traditional lithographic techniques.⁵⁵ Artificially separated SAMs allow for the creation of chemically patterned films not possible with other processing methods.⁵⁶

Microcontact printing, a common soft-lithography technique, applies onto a substrate an elastomeric stamp that is coated with the molecules to be patterned. The molecules transfer from the stamp to the substrate only where the stamp and the substrate come in contact.^{7,57-59} This patterning technique is limited to molecules that have sufficiently strong intermolecular interactions and are not susceptible to lateral diffusion across the surface. Employing AD SAMs in conjunction with contact displacement, it is possible to pattern molecules with weak intermolecular interactions by employing *microdisplacement printing*.^{49,50} **Figure 8A** shows a schematic diagram of the microdisplacement printing process.

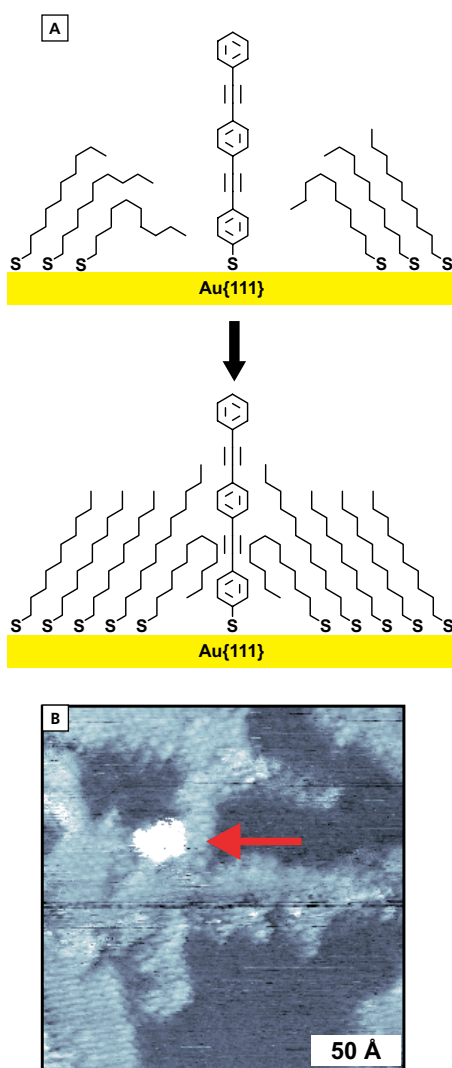


Figure 7. (A) 1-Dodecanethiol Vapor-Phase Annealing of an Oligo(Phenylene Ethynylene) Molecule Inserted into a Preformed 1-Dodecanethiolate SAM on a Au{111} Substrate. (B) STM Image ($V_{\text{sample}} = -1.0$ V, $I_{\text{tunnel}} = 5$ pA, $200 \text{ \AA} \times 200 \text{ \AA}$) of 1-Dodecanethiol Vapor-Phase Annealed into a 1-Decanethiolate SAM on a Au{111} Substrate That Was Inserted with Oligo(Phenylene Ethynylene) Molecules. The More Protruding Lattice Is Attributed to 1-Dodecanethiolate and the Less Protruding One to 1-Decanethiolate. The Red Arrow Indicates the Single Oligo(Phenylene Ethynylene) Molecule.

Initially, a single-component AD SAM was formed on a gold substrate. Subsequently, an elastomeric stamp coated with the molecules to be patterned was brought in contact with the substrate possessing the AD SAM; the molecules on the stamp transferred to the substrate in places where the stamp and substrate came in contact. The AD SAM was labile enough to be displaced by the molecules to be patterned through competitive adsorption, which resulted in patterned regions of both AD and the subsequently patterned molecules. **Figure 8B** is an LFM image of a patterned Au{111} substrate fabricated by microdisplacement printing. The low-friction squares (shown as dark) were attributed to the stamped C8 molecules, and the high-friction background (shown as light) to the preformed AD SAM. This molecular pattern combination was not possible with microcontact printing because of the high mobility of C8.^{59,60}

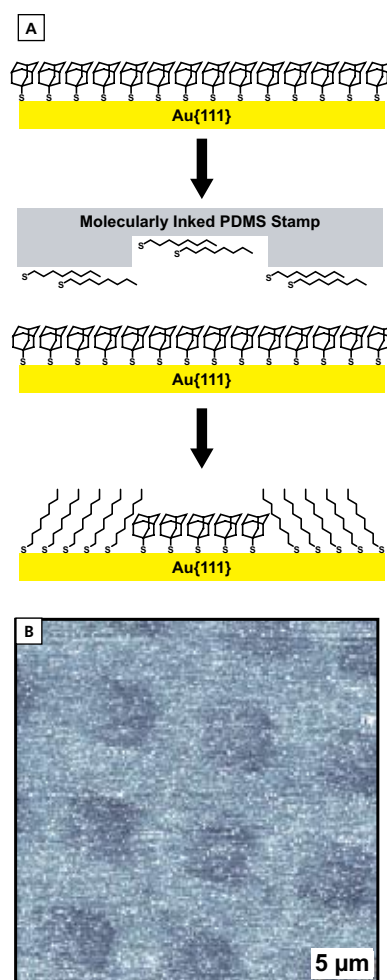


Figure 8. (A) Microdisplacement Printing Where a Preformed 1-Adamantanethiolate SAM Was Contacted with a Molecularly Coated Elastomeric Stamp. The Molecules to Be Patterned (1-Octanethiol) Displaced the 1-Adamantanethiol Molecules in Places Where the Stamp and Substrate Were in Contact. (B) Lateral Force Microscopy Image ($30 \text{ \mu m} \times 30 \text{ \mu m}$, Scan Rate = 1.0 Hz, Force Setpoint = 1.0 nN) of a Patterned Au{111} Substrate Fabricated by Microdisplacement Printing, Showing the Presence of Two Molecules on the Surface. The Low-Friction Squares (Shown as Dark) are the Stamped 1-Octanethiol Molecules, and the High-Friction Background (Shown as Light) is the Preformed 1-Adamantanethiolate SAM.

Microdisplacement printing increased the library of patternable molecules and the precision of soft-lithography techniques as compared to microcontact printing by hindering the diffusion of the stamped molecules across the substrate both during and following the stamping process. By hindering the diffusion of the stamped molecules during the stamping process, it was possible to pattern molecules with low intermolecular interactions by blocking the lateral motion of the molecules. Microcontact printing often requires solvent exposure to prevent the degradation of the patterned film over time due to diffusion across the surface. Solvent exposure also reduces the precision of the patterned structures due to molecular exchange. With microdisplacement printing, solvent exposure is not required because AD molecules are still present in places where the stamp did not contact the surface. Additionally, multiple stamping steps can be used to produce proximate structures, circumventing the difficulty of precise registration of neighboring patterns in conventional soft-lithography techniques.⁵⁰

Coadsorption techniques and *n*-alkanethiols of varied intermolecular-interaction strengths have been utilized to understand and control the thiol-transport mechanism in dip-pen nanolithography. *Dip-pen nanolithography* directly writes molecular inks from an atomic-force-microscope tip onto a surface.^{61,62} Salaita et al. fabricated microscopically phase-separated monolayers employing cantilever tips that were inked with two molecules.⁶³ When the chemical structures were patterned, the more hydrophilic *n*-alkanethiol formed the interior phase, and the more hydrophobic *n*-alkanethiols formed the outer phase. To understand the ink transport mechanism, Hampton et al. fabricated surface structures by patterning 1-octadecanethiol (C18, hydrophobic) and 16-mercaptohexadecanoic acid (MHDA,

hydrophilic) sequentially.⁶⁴ **Figure 9** depicts the proposed mechanism of the sequential double-ink experiments. When MHDA was patterned atop a C18 SAM, the water meniscus was compact, resulting in a lower transport rate of the MHDA molecules. In contrast, when C18 was patterned atop an MHDA SAM, the water meniscus was spread out, resulting in a higher transport rate of the C18 molecules. This double-ink study demonstrated that the rate and direction of transport, as well as the ability of the molecular ink to pattern, are affected by the chemical functionality of the surface.⁶⁴

Chemically patterned structures can be further manipulated by employing *electrochemical desorption*.^{65–70} We employed electrochemical desorption in conjunction with coadsorption, postadsorption, and displacement processing techniques to fabricate separated SAMs of molecules that cannot endure other chemical processing techniques. This is especially useful for biomolecules, where the bioactivity of the molecule needs to be preserved after patterning. Separated SAMs of C8 and C12 were fabricated to demonstrate this technique.⁵⁶ **Figure 10A** outlines the fabrication of artificially separated C12-and-C8 SAMs. Initially, a separated C12-and-AD SAM was fabricated by solution displacement of a preformed AD SAM on a Au{111} substrate. Subsequently, the sample was immersed in a solution of C8, thereby producing self-assembled monolayers with separated domains of C12 and C8. **Figure 10B** is an STM image of an artificially separated C12 (more protruding lattice) and C8 (less protruding lattice) SAM fabricated by electrochemical desorption and replacement.⁴¹ The C12 domains remained intact, although smaller, throughout the electrochemical processing, and the C8 molecules adsorbed in regions where the gold surface was exposed.

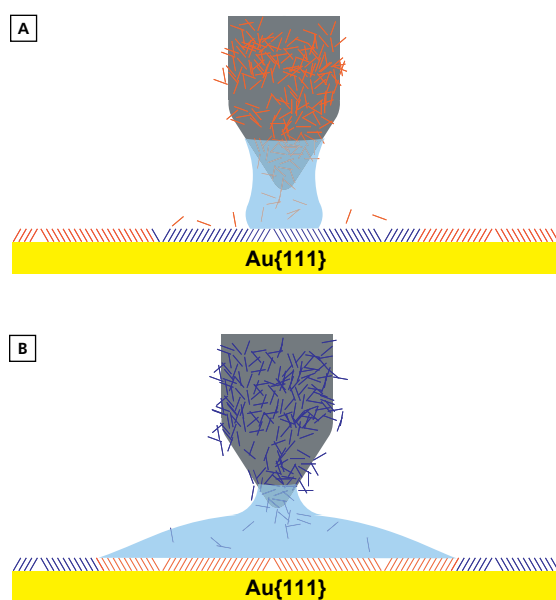


Figure 9. Schematic of the Double-Ink, Dip-Pen Nanolithography Experiments. **(A)** The Water Meniscus Was Compact When 16-Mercaptohexadecanoic Acid (MHDA) Molecules (Red) Were Patterned atop a 1-Octadecanethiolate SAM (Blue), Which Resulted in a Lower Transport Rate of the MHDA Molecules. **(B)** The Water Meniscus Was Spread Out When 1-Octadecanethiol Molecules (Blue) Were Patterned atop an MHDA SAM (Red), Which Resulted in a Higher Transport Rate of the 1-Octadecanethiol Molecules.

4.3. Tether and Capture of Biomolecules

By employing chemical processing techniques, it is possible to construct monolayer films that selectively capture large biomolecules, such as receptor proteins and antibodies, that specifically recognize small-molecule binding partners. This type of film can be used to elucidate molecular interactions between known proteins and their small-molecule targets, as well as to identify unknown proteins that bind to specific small molecules.⁷¹

Figure 11A shows a schematic of the solution insertion of the precursor tether molecule 23-(9-mercaptononyl)-3,6,9,12,15,18,21-heptaacosanoic acid [a carboxylic acid terminated oligo(ethylene glycol) *n*-alkanethiol] into a preformed 11-(9-mercaptononyl)-3,6,9-trioxaundecanol [a hydroxyl-terminated oligo(ethylene glycol) *n*-alkanethiolate] SAM. The solution insertion time was tailored to ensure optimal dilution of the tether molecules into the existing SAM. If tether molecules that are later functionalized with small-molecule probes are spaced too closely, nonspecific binding increases; if these derivatized tethers are spaced too far apart, then the efficiency of capturing large biomolecules is diminished. In the specific example shown in Figure 11A, the isolated precursor tether molecules were then functionalized with the small-molecule neurotransmitter serotonin (5-hydroxytryptamine, 5-HT) via EDC/NHS coupling chemistry.⁷² **Figure 11B** shows a schematic of how serotonin antibodies specifically recognize and bind to the 5-HT-functionalized tether molecules. In additional experiments, we have shown that antibodies selective for other closely related small molecules are not captured by serotonin-functionalized surfaces. Thus, this system demonstrates that small-molecule-derivatized surfaces can be fabricated and patterned at the molecular level to

optimize biospecific recognition. Furthermore, this approach is being adapted and applied to other important neurotransmitters and additional small molecules of analytical and medical importance.⁷³

5. Conclusions

In summary, we have fabricated chemically patterned structures with high precision and functionality by exploiting molecules with a range of intermolecular forces and employing an array of chemical patterning techniques. We designed specific postadsorption techniques to isolate, to manipulate, and to characterize single-molecule switches and other functional molecules. The stochastic switching activity of OPE molecules was controlled by manipulating their intermolecular interactions, as well as those of the surrounding matrix. The selective and

optimized capture of biomolecules has also been demonstrated by appropriately functionalized and tailored surfaces.

Exploiting the labile nature of AD SAMs, chemical patterning techniques were enhanced by hindering the lateral movement of molecules across a patterned surface, and the difficulty in the precise registration of adsorbates was avoided. By tuning the intermolecular-interaction strengths of molecular inks, we elucidated the transport mechanism of *n*-alkanethiolate molecules on a functionalized surface in dip-pen nanolithography.

We also fabricated artificially separated SAMs employing electrochemical processing techniques, otherwise not possible by coadsorption methods. This approach can be used to isolate molecules that cannot withstand chemical processing techniques.

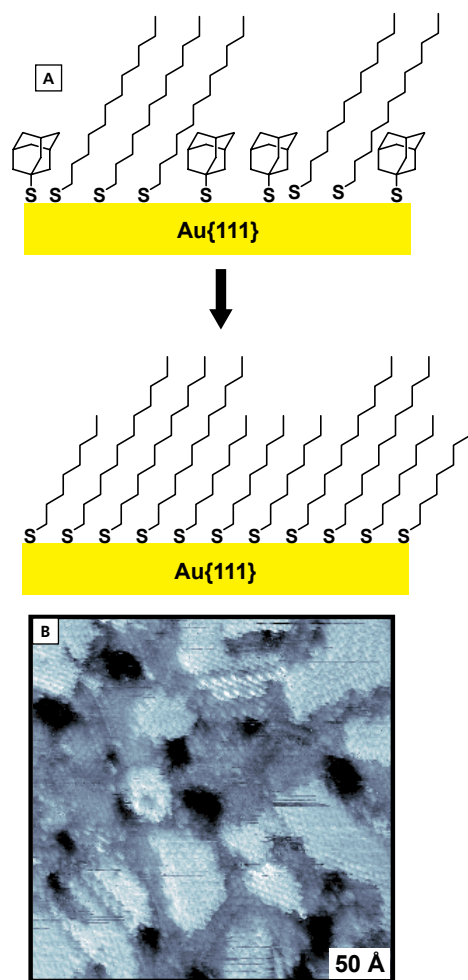


Figure 10. (A) The Fabrication of an Artificially Separated SAM. Initially, the 1-Adamantanethiolate Lattice of a Separated 1-Dodecanethiolate and 1-Adamantanethiolate SAM Was Desorbed Selectively from the Surface. Subsequently, 1-Octanethiol Molecules Were Adsorbed onto the Exposed Surface, Forming the Artificially Separated 1-Dodecanethiolate and 1-Octanethiolate SAM. (B) STM Image ($V_{\text{sample}} = -1.0$ V, $I_{\text{tunnel}} = 1$ pA, $300 \text{ \AA} \times 300 \text{ \AA}$) of an Artificially Separated 1-Dodecanethiolate and 1-Octanethiolate SAM on a Au{111} Substrate Showing the Two Distinct Domains of Molecules. The More Protruding Domains Are Attributed to 1-Dodecanethiolate and the Less Protruding Ones to 1-Octanethiolate.

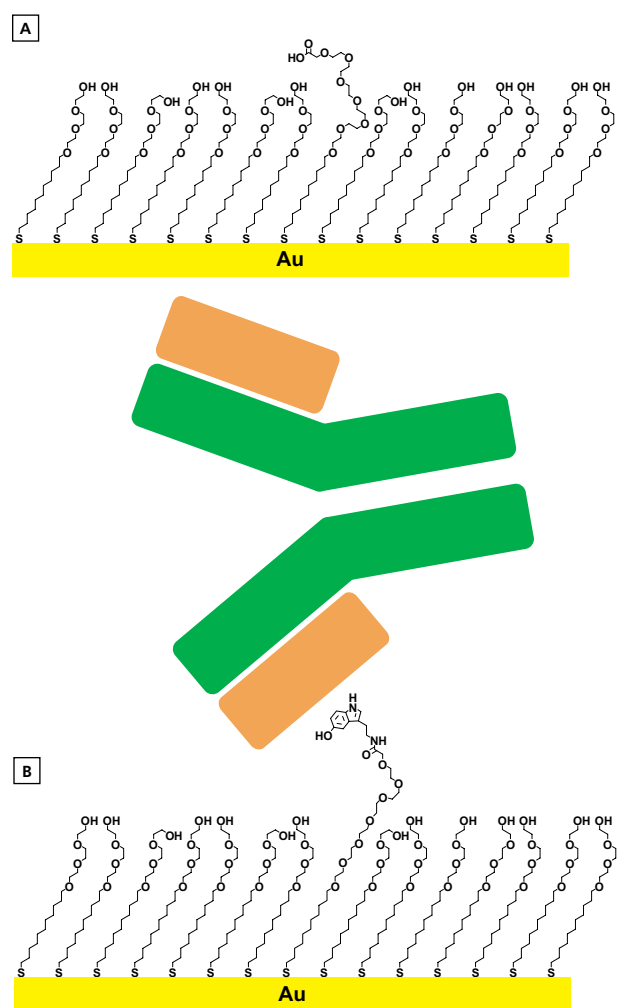


Figure 11. (A) The Solution Insertion of Precursor Tether Molecules [Carboxylic Acid Terminated, Oligo(Ethylene Glycol) Functionalized *n*-Alkanethiols] into a Preformed Oligo(Ethylene Glycol) Functionalized *n*-Alkanethiolate SAM. (B) The Capture of a Serotonin Antibody by the 5-HTP Functionalized Tether Molecule.

6. Acknowledgments

The authors thank Dr. Mary Elizabeth Anderson, Adam Kurland, Mitchell Shuster, and Dr. Matthew Szapacs for helpful and insightful discussions; and Amanda Moore, and Drs. Jason Monnell, Dan Fuchs, and Penelope Lewis for analytical assistance. The Air Force Office of Scientific Research, Army Research Office, Defense Advanced Research Projects Agency, National Science Foundation, Office of Naval Research, Semiconductor Research Corporation, and Sigma-Aldrich Corporation are gratefully acknowledged for their financial support. Much of this work was done as a part of the National Science Foundation supported Center for Nanoscale Science, a Materials Research Science and Engineering Center, and the Penn State node of the National Nanofabrication Infrastructure Network, a national resource for chemically advanced nanolithography.

7. References and Notes

- (1) Kasemo, B. *Surf. Sci.* **2002**, *500*, 656.
- (2) Mantooh, B. A.; Weiss, P. S. *Proc. IEEE* **2003**, *91*, 1785.
- (3) Tirrell, M.; Kokkoli, E.; Biesalski, M. *Surf. Sci.* **2002**, *500*, 61.
- (4) *Microolithography*; Rai-Choudhury, P., Ed.; Handbook of Microolithography, Micromachining, and Microfabrication, Vol. 1; SPIE Optical Engineering Press: Bellingham, WA, 1997.
- (5) Adamson, A. W.; Gast, A. P. *Physical Chemistry of Surfaces*, 6th ed.; Wiley: New York, 1997.
- (6) Allara, D. L.; Nuzzo, R. G. *Langmuir* **1985**, *1*, 52.
- (7) Laibinis, P. E.; Fox, M. A.; Folkers, J. P.; Whitesides, G. M. *Langmuir* **1991**, *7*, 3167.
- (8) Laibinis, P. E.; Nuzzo, R. G.; Whitesides, G. M. *J. Phys. Chem.* **1992**, *96*, 5097.
- (9) Nuzzo, R. G.; Dubois, L. H.; Allara, D. L. *J. Am. Chem. Soc.* **1990**, *112*, 558.
- (10) Piner, R. D.; Hong, S.; Mirkin, C. A. *Langmuir* **1999**, *15*, 5457.
- (11) Poirier, G. E. *Chem. Rev.* **1997**, *97*, 1117.
- (12) Wilbur, J. L.; Biebuyck, H. A.; MacDonald, J. C.; Whitesides, G. M. *Langmuir* **1995**, *11*, 825.
- (13) Lewis, P. A.; Donhauser, Z. J.; Mantooh, B. A.; Smith, R. K.; Bumm, L. A.; Kelly, K. F.; Weiss, P. S. *Nanotechnology* **2001**, *12*, 231.
- (14) Love, J. C.; Estroff, L. A.; Kriebel, J. K.; Nuzzo, R. G.; Whitesides, G. M. *Chem. Rev.* **2005**, *105*, 1103.
- (15) Smith, R. K.; Lewis, P. A.; Weiss, P. S. *Prog. Surf. Sci.* **2004**, *75*, 1.
- (16) Xia, Y.; Rogers, J. A.; Paul, K. E.; Whitesides, G. M. *Chem. Rev.* **1999**, *99*, 1823.
- (17) Ulman, A. *Chem. Rev.* **1996**, *96*, 1533.
- (18) Dubois, L. H.; Nuzzo, R. G. *Annu. Rev. Phys. Chem.* **1992**, *43*, 437.
- (19) Dubois, L. H.; Zegarski, B. R.; Nuzzo, R. G. *J. Chem. Phys.* **1993**, *98*, 678.
- (20) Poirier, G. E.; Pylant, E. D. *Science* **1996**, *272*, 1145.
- (21) Poirier, G. E.; Tarlov, M. J. *J. Phys. Chem.* **1995**, *99*, 10966.
- (22) Schlenoff, J. B.; Li, M.; Ly, H. J. *Am. Chem. Soc.* **1995**, *117*, 12528.
- (23) Delamarche, E.; Michel, B.; Gerber, C.; Anselmetti, D.; Güntherodt, H.-J.; Wolf, H.; Ringsdorf, H. *Langmuir* **1994**, *10*, 2869.
- (24) Clegg, R. S.; Hutchison, J. E. *J. Am. Chem. Soc.* **1999**, *121*, 5319.
- (25) Clegg, R. S.; Hutchison, J. E. *Langmuir* **1996**, *12*, 5239.
- (26) Clegg, R. S.; Reed, S. M.; Smith, R. K.; Barron, B. L.; Rear, J. A.; Hutchison, J. E. *Langmuir* **1999**, *15*, 8876.
- (27) Lewis, P. A.; Smith, R. K.; Kelly, K. F.; Bumm, L. A.; Reed, S. M.; Clegg, R. S.; Gunderson, J. D.; Hutchison, J. E.; Weiss, P. S. *J. Phys. Chem. B* **2001**, *105*, 10630.
- (28) Smith, R. K.; Reed, S. M.; Lewis, P. A.; Monnell, J. D.; Clegg, R. S.; Kelly, K. F.; Bumm, L. A.; Hutchison, J. E.; Weiss, P. S. *J. Phys. Chem. B* **2001**, *105*, 1119.
- (29) Nowacki, W.; Hedberg, K. W. *J. Am. Chem. Soc.* **1948**, *70*, 1497.
- (30) Dameron, A. A. Controlling Molecular Assemblies. Ph.D. Thesis, The Pennsylvania State University, University Park, PA, May 2006.
- (31) Dameron, A. A.; Charles, L. F.; Weiss, P. S. *J. Am. Chem. Soc.* **2005**, *127*, 8697.
- (32) Monnell, J. D.; Stapleton, J. J.; Jackiw, J. J.; Dunbar, T.; Reinert, W. A.; Dirk, S. M.; Tour, J. M.; Allara, D. L.; Weiss, P. S. *J. Phys. Chem. B* **2004**, *108*, 9834.
- (33) Bain, C. D.; Biebuyck, H. A.; Whitesides, G. M. *Langmuir* **1989**, *5*, 723.
- (34) Folkers, J. P.; Laibinis, P. E.; Whitesides, G. M. *Langmuir* **1992**, *8*, 1330.
- (35) Bain, C. D.; Whitesides, G. M. *J. Am. Chem. Soc.* **1989**, *111*, 7164.
- (36) Stranick, S. J.; Parikh, A. N.; Tao, Y.-T.; Allara, D. L.; Weiss, P. S. *J. Phys. Chem.* **1994**, *98*, 7636.
- (37) Monnell, J. D. Molecular-Scale Properties of Functional Materials and Molecules. Ph.D. Thesis, The Pennsylvania State University, University Park, PA, February 2005.
- (38) Stranick, S. J.; Atre, S. V.; Parikh, A. N.; Wood, M. C.; Allara, D. L.; Winograd, N.; Weiss, P. S. *Nanotechnology* **1996**, *7*, 438.
- (39) These molecules were too long to allow the molecular lattice of the SAM to be resolved.
- (40) Bumm, L. A.; Arnold, J. J.; Dunbar, T. D.; Allara, D. L.; Weiss, P. S. *J. Phys. Chem. B* **1999**, *103*, 8122.
- (41) The depressed regions are attributed to substrate vacancy islands created during the self-assembled monolayer formation process.
- (42) Monnell, J. D.; Stapleton, J. J.; Dirk, S. M.; Reinert, W. A.; Tour, J. M.; Allara, D. L.; Weiss, P. S. *J. Phys. Chem. B* **2005**, *109*, 20343.
- (43) Donhauser, Z. J.; Price, D. W., II; Tour, J. M.; Weiss, P. S. *J. Am. Chem. Soc.* **2003**, *125*, 11462.
- (44) Cygan, M. T.; Dunbar, T. D.; Arnold, J. J.; Bumm, L. A.; Shedlock, N. F.; Burgin, T. P.; Jones, L., II; Allara, D. L.; Tour, J. M.; Weiss, P. S. *J. Am. Chem. Soc.* **1998**, *120*, 2721.
- (45) Bumm, L. A.; Arnold, J. J.; Charles, L. F.; Dunbar, T. D.; Allara, D. L.; Weiss, P. S. *J. Am. Chem. Soc.* **1999**, *121*, 8017.
- (46) Donhauser, Z. J.; Mantooh, B. A.; Kelly, K. F.; Bumm, L. A.; Monnell, J. D.; Stapleton, J. J.; Price, D. W., Jr.; Rawlett, A. M.; Allara, D. L.; Tour, J. M.; Weiss, P. S. *Science* **2001**, *292*, 2303.
- (47) Donhauser, Z. J.; Mantooh, B. A.; Pearl, T. P.; Kelly, K. F.; Nanayakkara, S. U.; Weiss, P. S. *Jpn. J. Appl. Phys., Part 1* **2002**, *41*, 4871.
- (48) Weck, M.; Jackiw, J. J.; Rossi, R. R.; Weiss, P. S.; Grubbs, R. H. *J. Am. Chem. Soc.* **1999**, *121*, 4088.
- (49) Dameron, A. A.; Hampton, J. R.; Smith, R. K.; Mullen, T. J.; Gillmor, S. D.; Weiss, P. S. *Nano Lett.* **2005**, *5*, 1834.
- (50) Dameron, A. A.; Hampton, J. R.; Gillmor, S. D.; Hohman, J. N.; Weiss, P. S. *J. Vac. Sci. Technol. B* **2005**, *23*, 2929.
- (51) Bumm, L. A.; Arnold, J. J.; Cygan, M. T.; Dunbar, T. D.; Burgin, T. P.; Jones, L., II; Allara, D. L.; Tour, J. M.; Weiss, P. S. *Science* **1996**, *271*, 1705.
- (52) Lewis, P. A.; Inman, C. E.; Maya, F.; Tour, J. M.; Hutchison, J. E.; Weiss, P. S. *J. Am. Chem. Soc.* **2005**, *127*, 17421.
- (53) Lewis, P. A.; Inman, C. E.; Yao, Y.; Tour, J. M.; Hutchison, J. E.; Weiss, P. S. *J. Am. Chem. Soc.* **2004**, *126*, 12214.
- (54) Moore, A. M.; Dameron, A. A.; Mantooh, B. A.; Smith, R. K.; Fuchs, D. J.; Cizek, J. W.; Maya, F.; Yao, Y.; Tour, J. M.; Weiss, P. S. *J. Am. Chem. Soc.* **2006**, *128*, 1959.
- (55) Xia, Y.; Whitesides, G. M. *Angew. Chem., Int. Ed.* **1998**, *37*, 550.
- (56) Mullen, T. J.; Dameron, A. A.; Weiss, P. S. *J. Phys. Chem. B* **2006**, *110*, 14410.
- (57) Wilbur, J. L.; Kumar, A.; Kim, E.; Whitesides, G. M. *Adv. Mater.* **1994**, *6*, 600.

- (58) Larsen, N. B.; Biebuyck, H.; Delamarche, E.; Michel, B. *J. Am. Chem. Soc.* **1997**, *119*, 3017.
- (59) Delamarche, E.; Schmid, H.; Bietsch, A.; Larsen, N. B.; Rothuizen, H.; Michel, B.; Biebuyck, H. *J. Phys. Chem. B* **1998**, *102*, 3324.
- (60) Libiouille, L.; Bietsch, A.; Schmid, H.; Michel, B.; Delamarche, E. *Langmuir* **1999**, *15*, 300.
- (61) Jaschke, M.; Butt, H.-J. *Langmuir* **1995**, *11*, 1061.
- (62) Piner, R. D.; Zhu, J.; Xu, F.; Hong, S.; Mirkin, C. A. *Science* **1999**, *283*, 661.
- (63) Salaita, K.; Amarnath, A.; Maspoch, D.; Higgins, T. B.; Mirkin, C. A. *J. Am. Chem. Soc.* **2005**, *127*, 11283.
- (64) Hampton, J. R.; Dameron, A. A.; Weiss, P. S. *J. Am. Chem. Soc.* **2006**, *128*, 1648.
- (65) Hobara, D.; Kakiuchi, T. *Electrochem. Commun.* **2001**, *3*, 154.
- (66) Hobara, D.; Ota, M.; Imabayashi, S.; Niki, K.; Kakiuchi, T. *J. Electroanal. Chem.* **1998**, *444*, 113.
- (67) Hobara, D.; Sasaki, T.; Imabayashi, S.; Kakiuchi, T. *Langmuir* **1999**, *15*, 5073.
- (68) Imabayashi, S.; Hobara, D.; Kakiuchi, T.; Knoll, W. *Langmuir* **1997**, *13*, 4502.
- (69) Kakiuchi, T.; Iida, M.; Gon, N.; Hobara, D.; Imabayashi, S.; Niki, K. *Langmuir* **2001**, *17*, 1599.
- (70) Kakiuchi, T.; Sato, K.; Iida, M.; Hobara, D.; Imabayashi, S.; Niki, K. *Langmuir* **2000**, *16*, 7238.
- (71) Szapacs, M. E. Understanding Neurodegeneration and Psychiatric Disease in Mouse Models: The Interaction Between Serotonin and Brain-Derived Neurotrophic Factor. Ph.D. Thesis, The Pennsylvania State University, University Park, PA, 2004.
- (72) Hermanson, G. T. *Bioconjugate Techniques*; Academic Press: San Diego, 1996.
- (73) Shuster, M. J.; Vaish, A.; Szapacs, M. E.; Anderson, M. E.; Weiss, P. S.; Andrews, A. M. The Pennsylvania State University, University Park, PA. Unpublished work, 2006.

About the Authors

Thomas J. Mullen is a Ph.D. candidate in chemistry under the direction of Professor Paul S. Weiss at The Pennsylvania State University. He received his B.S. degree in chemistry in 2003 from the University of Florida. In the summers of 2002 and 2003, he was an Office of Navy Research intern studying the dynamics of thin-film polymers with Dr. Kathy J. Wahl at the Naval Research Laboratory. Currently, Thomas is investigating self- and directed-assembly techniques of self-assembled monolayers in order to understand and to exploit their underlying processes and mechanisms with the aim of enhancing chemical patterning capabilities.

Arrelaine A. Dameron received her B.S. degree in creative studies in 2001 from the University of California at Santa Barbara. During her graduate research on molecular assemblies under the direction of Professor Paul S. Weiss at the Pennsylvania State University, she extensively investigated the self-assembly and directed patterning of 1-adamantanethiol before receiving her Ph.D. in January of 2006. Currently, Dr. Dameron is studying atomic layer deposition as a postdoctoral researcher with Professor Steven George at the University of Colorado in Boulder, Colorado.

Anne M. Andrews is an assistant professor of veterinary and biomedical sciences at The Pennsylvania State University (Penn State) and a member of Penn State's Neuroscience Institute and Molecular Toxicology Program. She received her B.S. degree in 1985 from Penn State and her Ph.D. in chemistry in 1993 from American University. Her thesis work on selective

neurotoxicity was conducted at the National Institute of Mental Health with Dr. Dennis L. Murphy, where she was an NIH predoctoral fellow, an NIH postdoctoral fellow, and ultimately a senior staff fellow.

Research in Professor Andrews's group is centered on the chemistry of the serotonin neurotransmitter system. The primary goal is to understand more fully the role of serotonin in complex behavior, and the etiology and treatment of psychiatric disorders (depression and anxiety) and neurodegenerative diseases (Alzheimer's and Parkinson's). Genetically engineered mice, as well as selective drugs and neurotoxins are used as tools to investigate normative behavior and disease processes. Neurochemistry in these model systems is studied using both in vivo and ex vivo bioanalytical techniques, which are also developed in her laboratories. Neurotransmitter-derivatized self-assembled monolayer "neurochips" recently have been designed to facilitate the development of novel biosensors and functionally directed proteomics.

Professor Andrews has been awarded an NIH Fellows Award for Research Excellence (1997), the American Parkinson's Disease Association Award (2001), and the Eli Lilly Outstanding Analytical Chemist Award (2001, 2002).

Paul S. Weiss is Distinguished Professor of Chemistry and Physics at The Pennsylvania State University, where he began his academic career as an assistant professor in 1989. He received his S.B. and S.M. degrees in chemistry from MIT in 1980 and his Ph.D. degree in chemistry from the University of California at Berkeley in 1986, having worked with Professor Yuan T. Lee on crossed-molecular-beam reactions of excited atoms. He was a postdoctoral member of the technical staff at Bell Laboratories (1986–1988) and a visiting scientist at IBM's Almaden Research Center (1988–1989). He was also a visiting professor at the University of Washington Department of Molecular Biotechnology (1996–1997), and at the Kyoto University Electronic Science and Engineering Department and Venture Business Laboratory (1998 and 2000).

Professor Weiss investigates the chemical, physical, optical, mechanical, and electronic properties of surfaces at the atomic scale. He and his students have developed new techniques to expand the applicability and chemical specificity of scanning probe microscopies and spectroscopies. They have applied these to the study of catalysis, self- and directed assembly, molecular- and nanoscale electronics, and single-molecule motors. They work to advance nanofabrication down to ever-smaller scales and greater chemical specificity in order to create test beds for molecular devices and platforms for sensors.

Since joining Penn State, Dr. Weiss has been awarded a National Science Foundation Presidential Young Investigator Award (1991–1996), the Scanning Microscopy International Presidential Scholarship (1994), the B. F. Goodrich Collegiate Inventors Award (1994), an Alfred P. Sloan Foundation Fellowship (1995–1997), the American Chemical Society Nobel Laureate Signature Award for Graduate Education in Chemistry (1996), a John Simon Guggenheim Memorial Foundation Fellowship (1997), and a National Science Foundation Creativity Award (1997–1999). He was elected a Fellow of the American Association for the Advancement of Science (2000) and of the American Physical Society (2002).